JOC The Journal of Organic Chemistry

Article

pubs.acs.org/joc

Computational Insights into the Rhodium(III)-Catalyzed Coupling of Benzamides and 1,6-Enynes via a Tunable Arylative Cyclization

Lijuan Du, Yilu Xu, Shengwen Yang, Juan Li,* and Xionghui Fu

Department of Chemistry, Jinan University, Huangpu Road West 601, Guangzhou, Guangdong 510632, P. R. China

Supporting Information

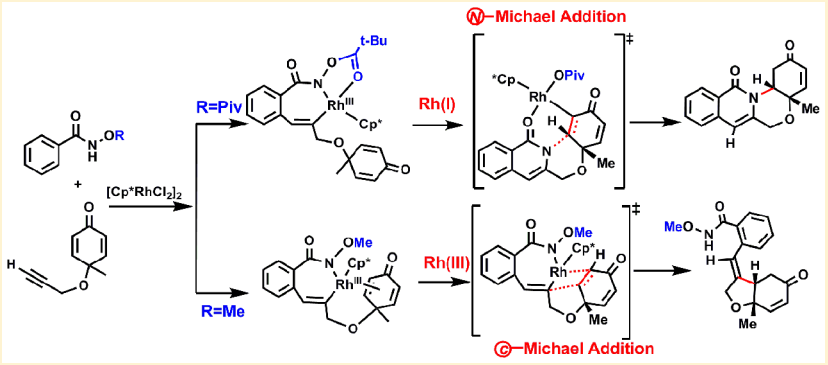

ABSTRACT: A density functional theory (DFT) study has been conducted to elucidate the mechanism of the rhodium(III)-catalyzed C−H activation of O-substituted *N*-hydroxybenzamides and cyclohexadienone-containing 1,6-enynes. The impact of different O-substituted internal oxidants (**OPiv** versus **OMe**) on the arylative cyclization (i.e., Ⓝ-Michael addition versus Ⓒ-Michael addition) has been evaluated in detail. The Ⓝ-Michael addition pathway proceeded via a Rh(I) species, while Rh(III) remained unchanged throughout the Ⓒ-Michael addition pathway. The Rh(III)/Rh(I) catalytic cycle in the Ⓝ-Michael addition pathway was different from those reported previously where the Rh(III)/Rh(V) catalytic cycle was favored for the Rh(III)-catalyzed C−H activation of O-substituted *N*-hydroxybenzamides. The first three steps were similar for the **OPiv**- and **OMe**-substituted substrates, which involved sequential N−H deprotonation, C−H activation (a concerted metalation−deprotonation process), and 1,6-enyne insertion steps. Starting from a seven-membered rhodacycle, the alternative mechanism would be controlled by the OR substituent. When the substituent was **OMe**, the unstable seven-membered rhodacycle was readily coordinated by a double bond of the cyclohexadienone which enabled the Ⓒ-Michael addition reaction. However, the presence of an **N-OPiv** moiety stabilized the seven-membered rhodacycle through a bidentate coordination which facilitated the Ⓝ-Michael addition process.

INTRODUCTION

The transition-metal-mediated activation of C−H bonds has become a potent tool in organic synthesis because it provides an effective and straightforward approach for the formation of new C−X bonds (X = C, N, O, S).[1] Among these transformations, research on the Rh(III)-catalyzed activation of C−H bonds, in particular, has grown rapidly over the past few years.[2] Several approaches have been developed to enhance the selectivity of C−H bond activation reactions, and one of the most common strategies involves the use of a directing group.[3] The use of a directing group that can also act as an internal oxidant has attracted considerable interest from numerous researchers because it represents an elegant and green synthetic strategy for the selective functionalization of C−H bonds that avoids the need for an additional oxidant.[4] Oxidizing directing groups reported to date for Rh-catalyzed activation of C−H bonds typically contain an N−O or N−N bond.[5]

Various cross-coupling partners, including alkenes, alkynes, allenes, imines, and a wide range of other unsaturated molecules, have been studied extensively in Rh-catalyzed C−H activation reactions.[6−8] Although significant progress has been achieved in this field during the past decade, there have been very few reports pertaining to the cyclohexadienone-containing 1,6-enynes.[9] The Rh(III)-catalyzed intramolecular C−H activation of O-substituted *N*-hydroxybenzamides **1** and cyclohexadienone-containing 1,6-enynes **2** was recently reported by Lin's group (Scheme 1).[9a] The use of different O-containing substituents (e.g., **OPiv** and **OMe**) on the directing group allowed for the formation of either tetracyclic isoquinolones **3a-OPiv** through an Ⓝ-Michael addition process or hydrobenzofurans **3b-OMe** through a Ⓒ-Michael addition process. Most notably, this work represented the first reported example of a Rh(III)-catalyzed arylative cyclization reaction involving a 1,6-enyne.

Received: December 2, 2015
Published: February 18, 2016

DOI: 10.1021/acs.joc.5b02747
J. Org. Chem. 2016, 81, 1921−1929

Scheme 1. Rh(III)-Catalyzed C−H Activation of O-Substituted *N*-Hydroxybenzamides with 1,6-Enynes as the Coupling Partner

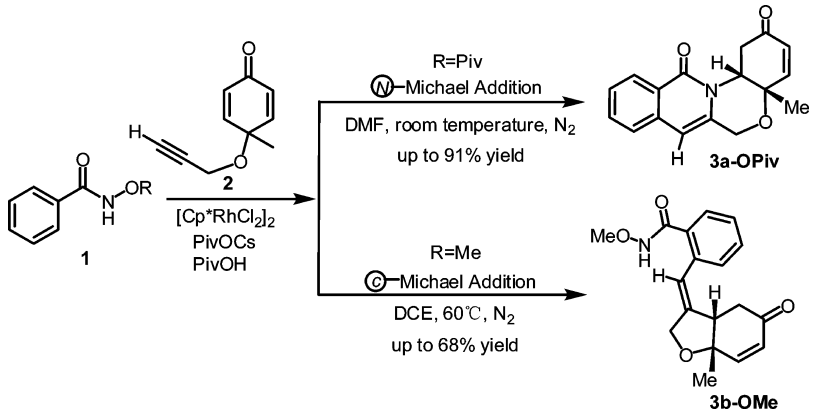

Scheme 2. Mechanism of Rh(III)-Catalyzed C−H Activation of O-Substituted *N*-Hydroxybenzamides with 1,6-Enynes as the Coupling Partner Proposed by Lin et al.

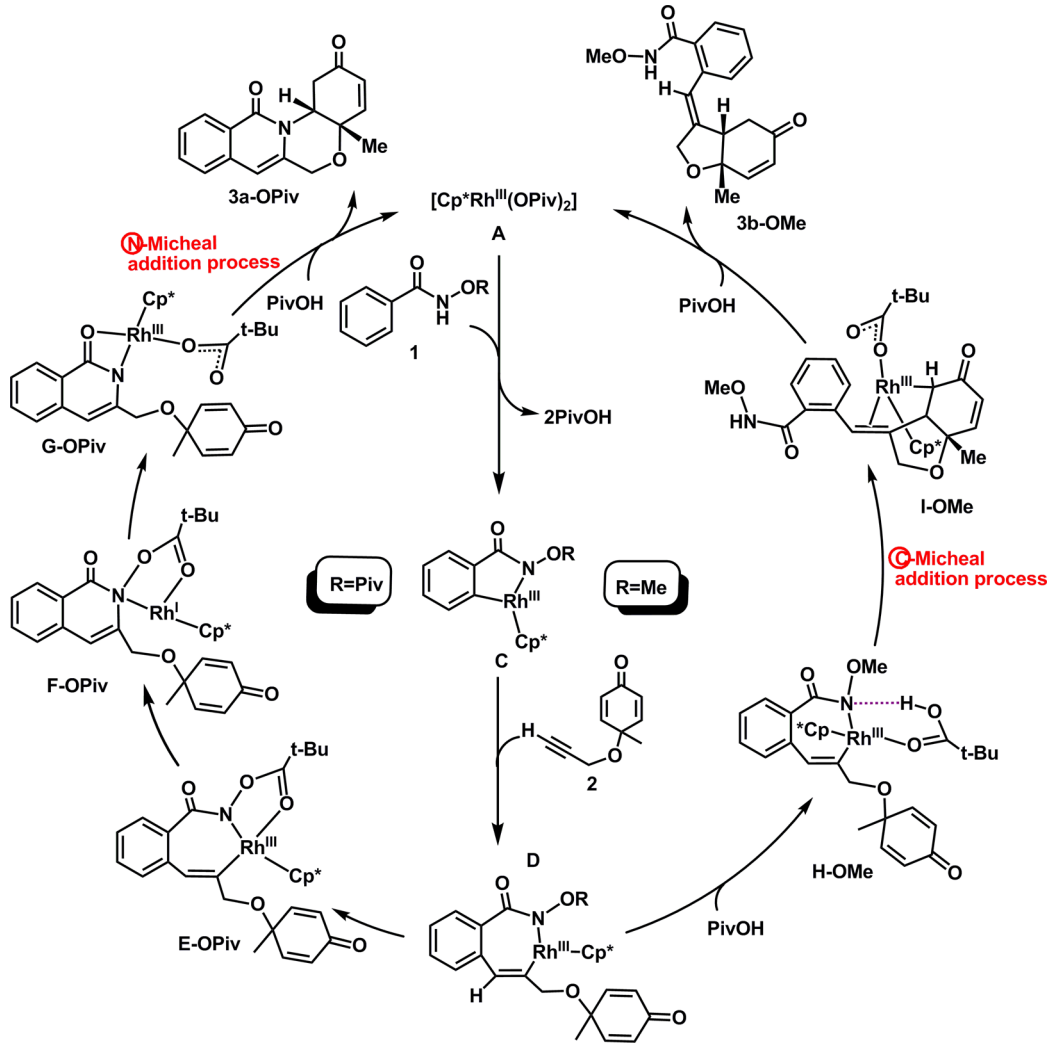

Lin's group[9a] proposed a mechanism to account for the Rh(III)-catalyzed C−H activation of O-substituted *N*-hydroxybenzamides and cyclohexadienone-containing 1,6-enynes, which is shown in Scheme 2. According to this mechanism, the steps involving the deprotonation of the amino group, the C−H cleavage, and insertion of the triple bond of the 1,6-enyne into the Rh−C bond would be similar for the **OPiv**- and **OMe**-substituted systems (**A** → **D-OMe** versus **A** → **D-OPiv**). Starting from the seven-membered rhodacycles **D-OMe** and **D-OPiv**, the mechanistic pathway would be controlled by the nature of the N-OR substituent. After the formation of **D-OPiv**, sequential C−N bond-forming reductive elimination and O−N cleavage steps would be accompanied by the intramolecular Ⓝ-Michael addition. Finally, a protonation mediated by PivOH

DOI: 10.1021/acs.joc.5b02747
J. Org. Chem. 2016, 81, 1921−1929

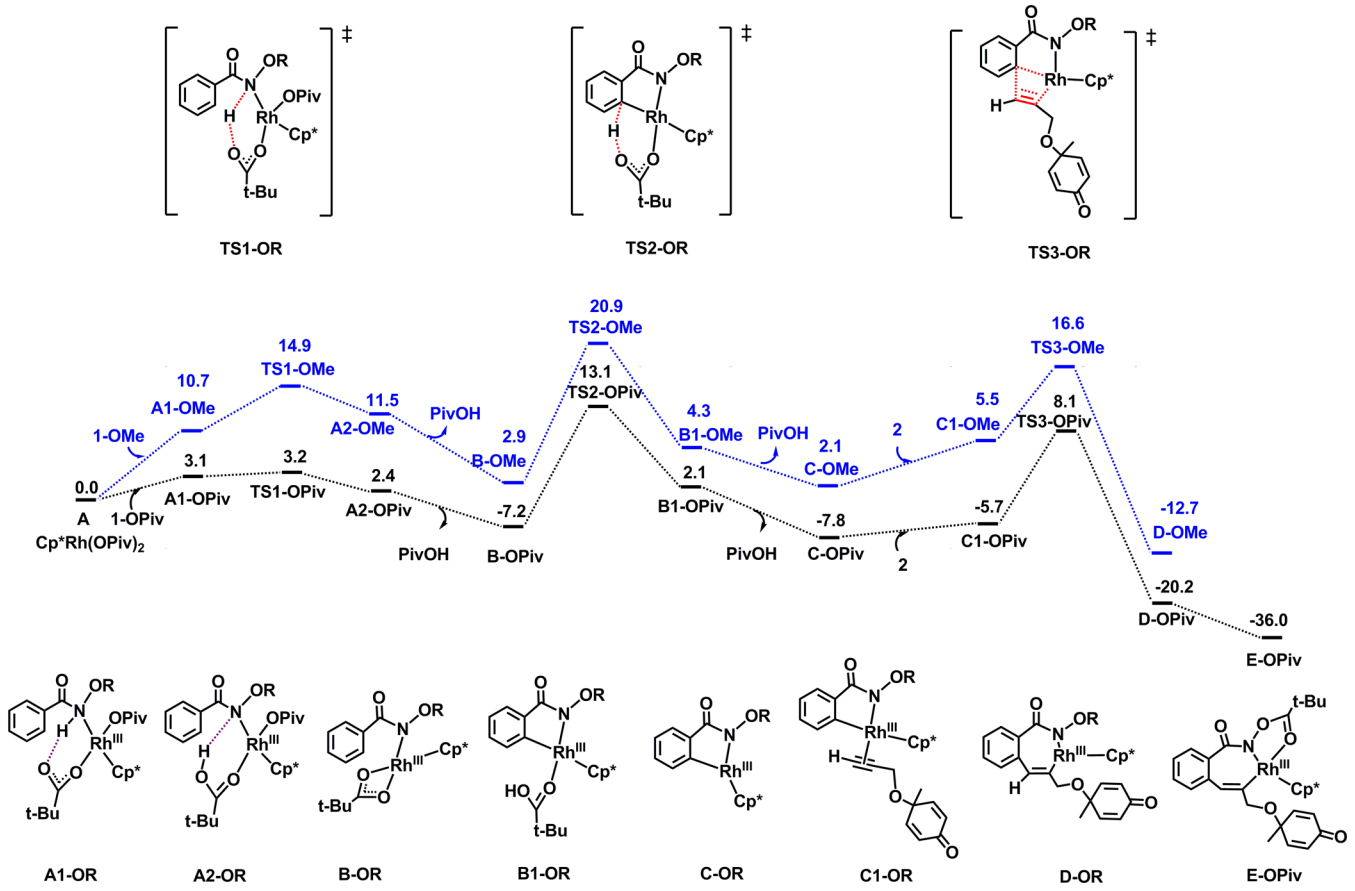

Figure 1. Free-energy profiles calculated for the coordination, N−H deprotonation, C−H activation, and 1,6-enyne insertion sequence for **A** → **E-OPiv** and **A** → **D-OMe**, respectively. The solvent-corrected free energies are given in kcal/mol (25 °C for the **OPiv** system and 60 °C for the **OMe** system).

would allow for the synthesis of the tetracyclic isoquinolone product **3a-OPiv** and regeneration of catalyst **A**. For the **OMe**-substituted system, the protonation of the seven-membered rhodacycle **D-OMe** by pivalic acid would afford the Rh(III) intermediate **H-OMe** which would enable the ©-Michael addition step. This step would provide access to the C−C coupling intermediate **I-OMe** which would be readily protonated by pivalic acid to regenerate **A** with the concomitant release of the desired hydrobenzofuran product **3b-OMe**.

Density functional theory (DFT) calculations[10] have recently been reported for the mechanism of the Rh-catalyzed C−H functionalization of O-substituted *N*-hydroxybenzamides with alkene, diazo, methylenecyclopropane, and cyclopropene substrates. The results of these calculations show that the N−O bond cleavage occurred via a Rh(III)/Rh(V) catalytic cycle. Further research efforts are therefore required to determine whether a Rh(V)-nitrene species is involved as a key intermediate for the Rh(III)-catalyzed C−H activation of O-substituted *N*-hydroxybenzamides with 1,6-enynes as the coupling partner.

Herein, we report our theoretical calculations toward developing a better understanding of the mechanisms involved in the Rh(III)-catalyzed coupling of benzamides and 1,6-enynes as well as our work toward delineating the factors that influence these reaction pathways. We have also provided a theoretical comparison of the reactions involving the two different substituents, **OPiv** and **OMe**, to explain why the **OPiv**-substituted system undergoes a Ⓝ-Michael addition while the **OMe**-substituted system undergoes a ©-Michael addition.

■ COMPUTATIONAL DETAILS

The molecular geometries of the complexes were optimized using DFT calculations at the M06 level.[11] Frequency calculations at the same level of theory were also performed to identify all of the stationary points as minima (zero imaginary frequencies) or transition states (one imaginary frequency) as well as to provide the free energies at 298.15 K. An IRC[12] analysis was performed to confirm that all of the stationary points were smoothly connected to each other. The Rh atom was described using the LANL2DZ basis set in addition to a double-valence basis set with the Hay and Wadt effective core potential.[13] Polarization functions were added for Rh (ζ_f = 1.350).[14] The 6-31G*[15] basis set was used for the other atoms. Single-point energy calculations were performed using the SMD model[16] for all of the gas phase optimized species to evaluate the solvent effects. DMF and DCE were used as the solvents for the **OPiv** and **OMe** systems, respectively, which correspond to the original experimental conditions. The SDD[17] and 6-311++G** basis sets were used in the SMD calculations for Rh and the other atoms, respectively. All of the calculations conducted in the current study were performed using the Gaussian 09 software packages.[18]

■ RESULTS AND DISCUSSION

According to Scheme 2, the **1-OPiv** (**OPiv**-substituted) and **1-OMe** (**OMe**-substituted) substrates both share similar N−H deprotonation, C−H activation, and 1,6-enyne insertion steps, although the resulting seven-membered rhodacycle intermediates progress down different reaction pathways. As shown in

DOI: 10.1021/acs.joc.5b02747
J. Org. Chem. 2016, 81, 1921−1929

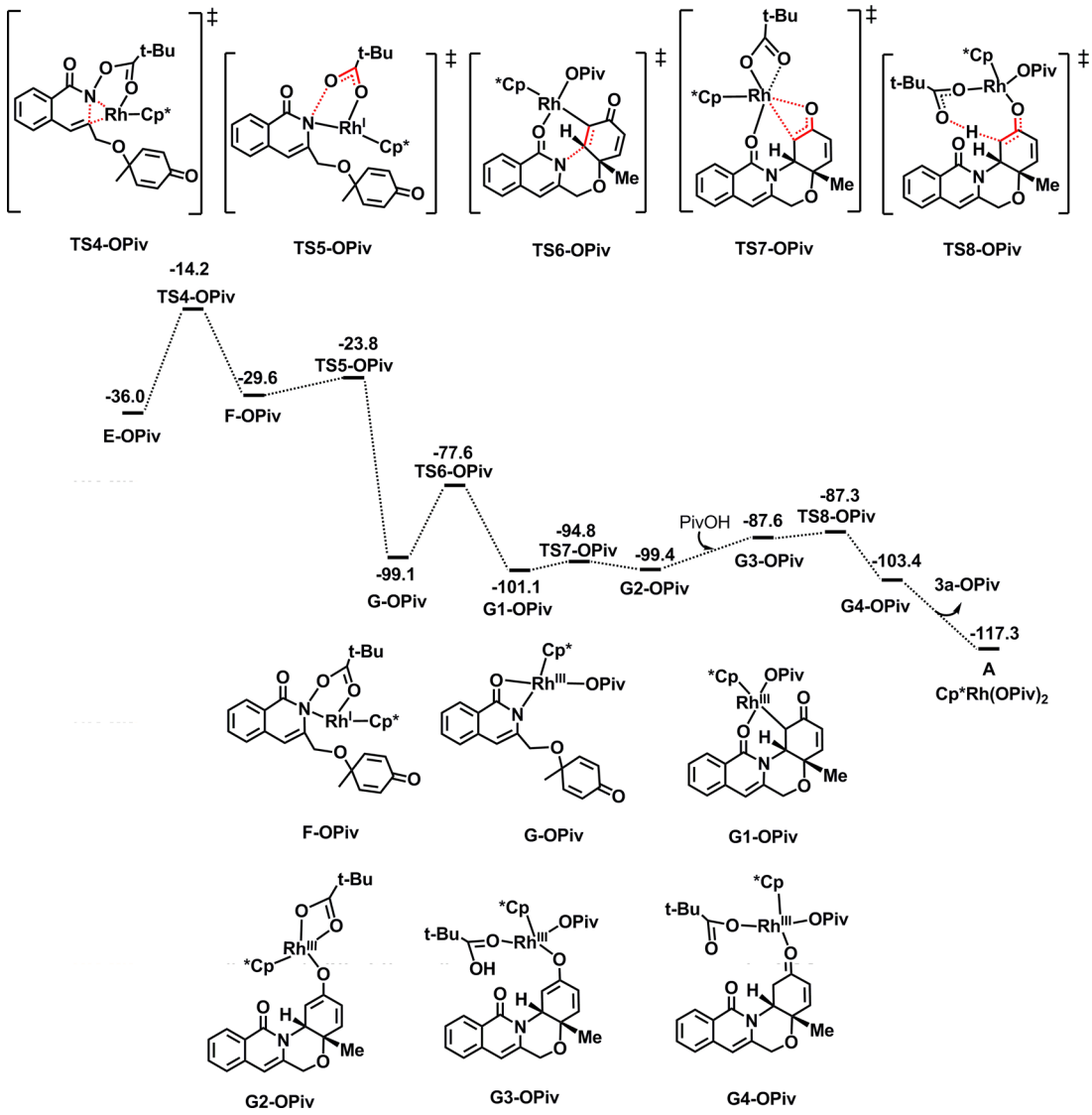

Figure 2. Free-energy profiles calculated for the Ⓝ-Michael addition pathway **E-OPiv** → **A**. The solvent-corrected free energies at 25 °C are given in kcal/mol.

Figure 1, the reactions of both substrates begin with the deprotonation of their amino groups followed by a concerted metalation−deprotonation (CMD) step to give rhodacycles **B1-OPiv** and **B1-OMe**. The subsequent removal of the neutral pivalic acid from **B1-OPiv** and **B1-OMe** results in the creation of a vacant coordination site on the Rh(III) center, which allows for the coordination of the 1,6-enyne substrate and the formation of **C1-OPiv** and **C1-OMe**, respectively. The subsequent insertion of the triple bond into the Rh−C bonds occurs via transition states **TS3-OPiv** and **TS3-OMe** to give the seven-membered rhodacycles **D-OPiv** and **D-OMe**, respectively. **D-OPiv** then undergoes a facile isomerization process to give the more stable **E-OPiv** species via the formation of a dative Rh−O bond (pivalic ligand).

Figure 2 shows the detailed mechanism for the formation of the final product **3a-OPiv** from **E-OPiv**. Starting from **E-OPiv**, a reductive elimination step via the three-membered ring transition state **TS4-OPiv** gives the Rh(I) species **F-OPiv**. The conversion of **E-OPiv** → **F-OPiv** has an energy barrier of 21.8 kcal/mol and is endergonic by 6.4 kcal/mol. The migration of the **OPiv** group from the N atom to the Rh atom occurs via the five-membered ring transition state **TS5-OPiv** to give the very stable Rh(III) species **G-OPiv**. The Ⓝ-Michael addition steps of **G-OPiv** then occurs to afford the C−N-coupled product **G1-OPiv** via the six-membered transition state **TS6-OPiv** with a free-energy barrier of 21.5 kcal/mol. The subsequent isomerization step for the formation of **G2-OPiv** involves the conversion of the Rh−C σ-bond to a Rh−O σ-bond. The coordination of a single molecule of PivOH to **G2-OPiv** leads to the formation of intermediate **G3-OPiv** which is followed by a proton migration step to give **G4-OPiv** via the transition state **TS8-OPiv**. Finally, the cleavage of the Rh−O dative bonds in **G4-OPiv** gives the final product **3a-OPiv**. On the basis of the results shown in Figures 1 and 2, it is clear that the reductive elimination and Ⓝ-Michael addition step is the rate-determining step for the **OPiv** system, and that the overall energy barrier for the pathway is 21.8 kcal/mol.

The calculated free-energy profiles for the Ⓒ-Michael addition pathway started from **D-OMe** are shown in Figure 3 and are hereafter referred to as path a. The coordination of a double bond of the cyclohexadienone to the Rh center leads to the formation of intermediate **D1-OMe**. Then, the Ⓒ-Michael

DOI: 10.1021/acs.joc.5b02747
J. Org. Chem. 2016, 81, 1921−1929

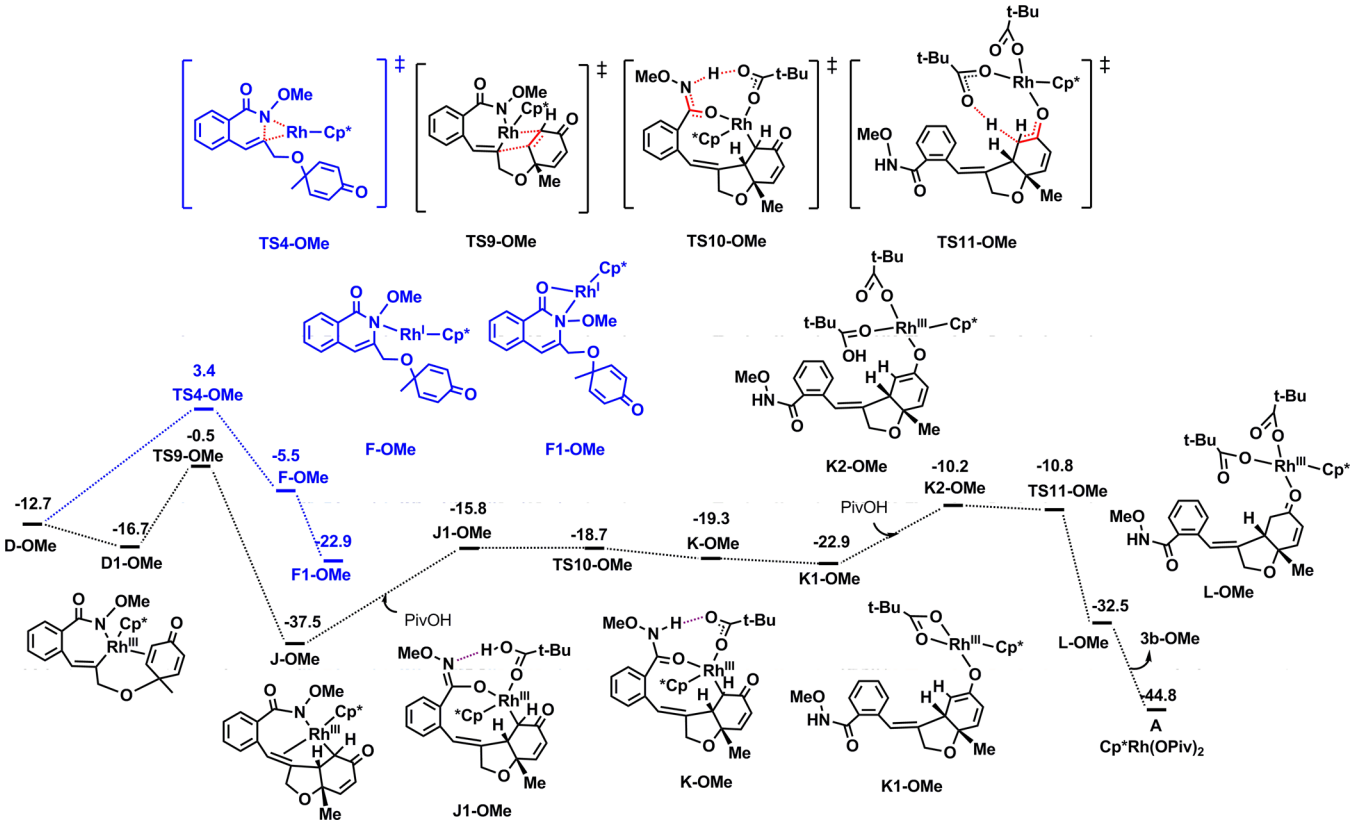

Figure 3. Free-energy profiles calculated for the ©-Michael addition pathway **D-OMe** → **A** based on path a and the ®-Michael addition pathway **D-OMe** → **E1-OMe**. The solvent-corrected free energies at 60 °C are given in kcal/mol.

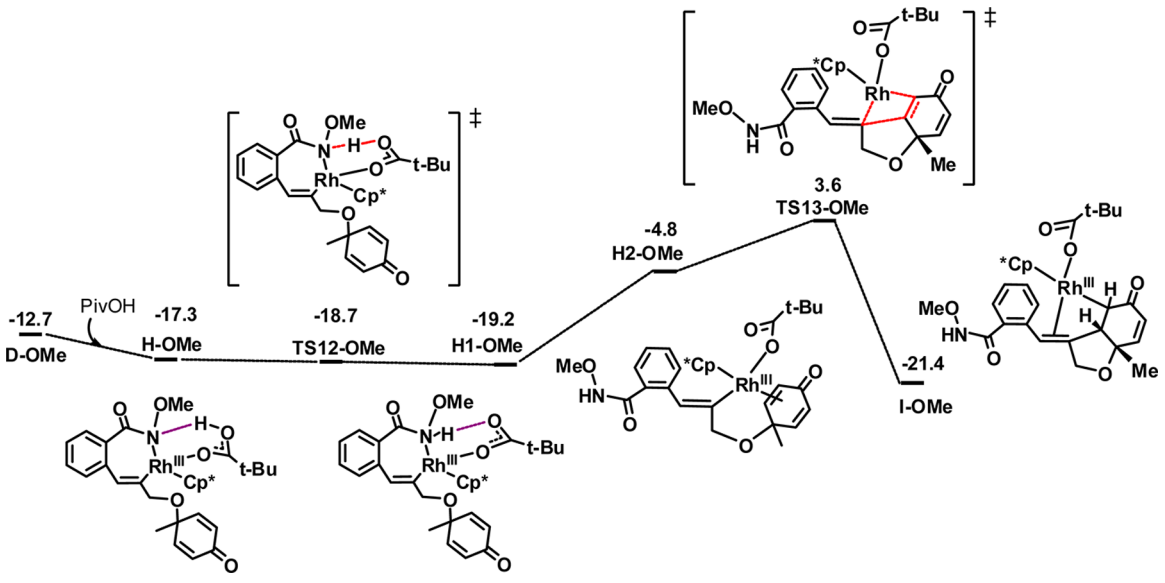

Figure 4. Free-energy profiles calculated for **D-OMe** → **I-OMe** based on path b (©-Michael addition pathway). The solvent-corrected free energies at 60 °C are given in kcal/mol.

addition occurs via transition state **TS9-OMe** with an energy barrier of 16.2 kcal/mol to give **J-OMe**. The subsequent coordination of a single molecule of PivOH to the Rh atom leads to the formation of **J1-OMe** which undergoes a H migration process from the PivOH ligand to the **OMe**-bonded nitrogen via **TS10-OMe** to give the Rh(III) intermediate **K-OMe**. Subsequently, **K-OMe** readily isomerizes to give the more stable species **K1-OMe** via the formation of a Rh−O σ-bond with the dissociation of the internal oxidant from the Rh center. The coordination of a single molecule of PivOH to the Rh center results in a change in the pivalate ligand from a bidentate to a monodentate ligand in **K2-OMe**. Finally, the pivalic-acid-mediated migration of a proton occurs to give **L-OMe** via **TS11-OMe** with the concomitant regeneration of the catalyst and the formation of the final product **3b-OMe**. The rate-determining transition state for this pathway is the proton

DOI: 10.1021/acs.joc.5b02747
J. Org. Chem. 2016, 81, 1921−1929

Scheme 3. Three ©-Michael Addition Pathways for the OPiv Species

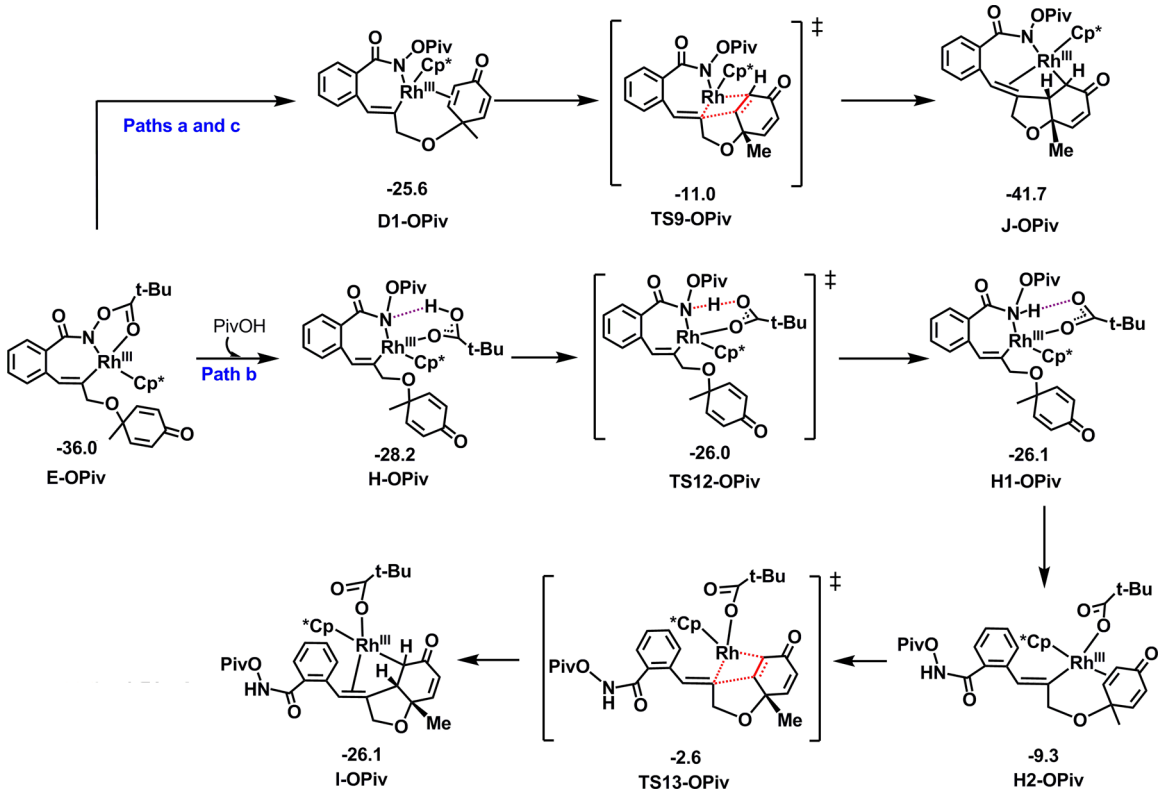

Scheme 4. C−N Reductive Elimination Step Starting from D-OR[a]

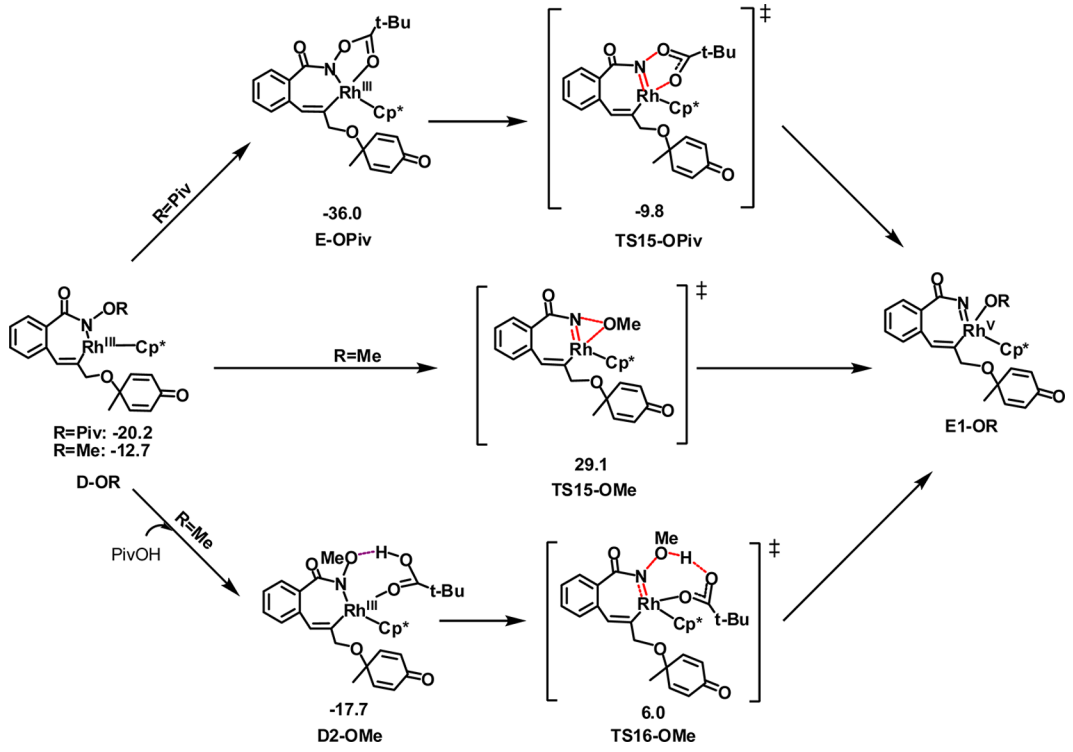

[a]The solvent-corrected relative free energies are shown in kcal/mol.

migration of **TS11-OMe**, which was determined to have an overall activation free-energy barrier of 27.3 kcal/mol.

Figure 4 shows the calculated free-energy profiles for the proposed mechanism of the ©-Michael addition shown in Scheme 2, which will be hereafter referred to as path b. The free energy of transition state **TS13-OMe** (3.6 kcal/mol) was determined to be higher than that of **TS9-OMe** (−0.5 kcal/mol). We also examined the alternative path c, where the

DOI: 10.1021/acs.joc.5b02747
J. Org. Chem. 2016, 81, 1921−1929

migration of a proton from PivOH to the keto-group-bonded carbon occurred prior to the protonation of the N atom of the internal oxidant after **J-OMe** (Figure S1 in the Supporting Information). However, the energy barrier for path c was determined to be 38.1 kcal/mol, which is 10.8 kcal/mol higher than that of path a. On the basis of these results, it is clear that the alternative pathways that include the ©-Michael addition can be eliminated. Starting from **D-OMe**, the pathway that includes the Ⓝ-Michael addition step is possible. However, the free energy of transition state **TS4-OMe** (3.4 kcal/mol) for the first reductive elimination step (Figure 3) was determined to be higher than that of **TS9-OMe** (−0.5 kcal/mol) and was therefore ruled out.

In a similar manner to the **OMe**-substituted substrate, we also calculated the three alternative pathways that include the ©-Michael addition step for the **OPiv** species (Scheme 3). However, the barrier for the first ©-Michael addition step in paths a and c was determined to be 25.0 kcal/mol. Path b would need to overcome an energy barrier of 33.4 kcal/mol. Therefore, the Ⓝ-Michael addition pathway (21.8 kcal/mol, Figure 2) would be kinetically favored over the ©-Michael addition pathway for the **OPiv**-substituted substrate.

It was envisaged that the migration of the **OPiv** and **OMe** groups from the N atoms of **E-OPiv** and **D-OMe** to the corresponding Rh atoms could precede the C−N reductive elimination steps to form the Rh(V) intermediates **E1-OPiv** and **E1-OMe**, respectively (Scheme 4). However, the transition states for these migration processes, **TS15-OPiv** and **TS15-OMe**, have much higher energy barriers of 26.2 and 41.8 kcal/mol, respectively, and are therefore ruled out. Further, while the energy barrier via **TS16-OMe** could be greatly lowered if one PivOH is involved, this barrier is still 2.6 kcal/mol higher than **TS4-OMe**. The calculations conducted in the current study for the **OPiv**-substituted *N*-hydroxybenzamides were different from those used in Xia's report,[10] where the Rh(III)/Rh(V) catalytic cycle was favored over the Rh(III)/Rh(I) cycle when an alkene, diazo, methylenecyclopropane, or cyclopropene species was used as the coupling partner. According to our calculations, the low energy reaction barrier for the C−N reductive elimination step **E-OPiv** → **F-OPiv** compared with the alkene, diazo, methylenecyclopropane, and cyclopropene substrates could be attributed to the availability of the additional π-bond of the 1,6-enyne.[19] As shown in Figure 5, the Rh−C1 bond distance of **TS4-OPiv** (2.064 Å) differed only slightly from that of **E-OPiv** (2.015 Å). This result implied that the effective coordination of the double bond to the Rh center in **TS4-OPiv** is maintained during the reductive elimination process.

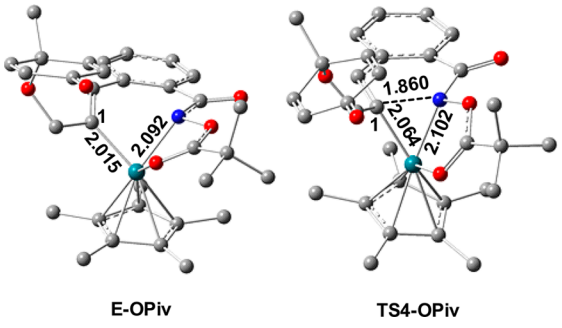

Figure 5. Structures of **E-OPiv** and **TS4-OPiv** with selected structural parameters and atomic numbering schemes. The hydrogen atoms have been omitted for clarity.

For the **OPiv** system, the rate-limiting step was the C−N bond-forming reductive elimination step with an energy barrier of 21.8 kcal/mol. For the **OMe** system, the transition state of the cyclohexadienone protonation step was rate limiting and the overall energy barrier was 27.3 kcal/mol. These overall barriers agreed well with the experimental observations that the Rh(III)-catalyzed C−H activation of **OPiv**-substituted substrate at 25 °C gave tetracyclic isoquinolone in 91% yield after 15 h, and the Rh(III)-catalyzed C−H activation of **OMe**-substituted substrate gave 63% yield of the hydrobenzofuran at 60 °C after 12 h.[9a] However, the rate-limiting step seems to contradict the conclusions of the kinetic isotope effect (KIE) study by Lin et al. (KIE = 6.1 for the **OPiv** system and KIE = 2.0 for the **OMe** system).[9a] For the **OPiv** system, the difference between the C−H bond activation barrier and the overall barrier was only 1.5 kcal/mol. One may question whether different computational methods affect the rate-limiting step. We attempted to calculate the C−H activation and C−N bond-forming reductive elimination steps by other computational methods.[20] However, the C−H activation step was not the rate-limiting step regardless of the method used. More studies, both experimental and theoretical, are needed to resolve the inconsistency.

It is noteworthy that the results of the reaction selectivity[21] are also consistent with the experimental observations.[9a] The reasons for the differences between the **OPiv**- and **OMe**-substituted systems are as follows: For the reaction of the **OPiv**-substituted substrate, the high stability of the seven-membered rhodacycle **E-OPiv** leads to a significant increase in the overall energy demand of the ©-Michael addition pathway, which would ultimately prevent it from occurring. For the **OMe**-substituted substrate, the unstable seven-membered rhodacycle **D-OMe** allows for the facile coordination of the double bond of the cyclohexadienone, thereby allowing the facile occurrence of the ©-Michael addition pathway. This rationale is also supported by the solvent effect in the experiment. The use of DCE instead of DMF as the solvent for the **OMe**-substituted substrate is explained by the coordinating ability of the solvent. The DMF solvent can act as a ligand to coordinate to Rh in **D-OMe** which blocks the formation of **D1-OMe** and thus disfavors the ©-Michael addition pathway.

CONCLUSIONS

The mechanism of the Rh(III)-catalyzed C−H activation of O-substituted *N*-hydroxybenzamides with cyclohexadienone-containing 1,6-enynes has been studied using density functional theory with the M06 method. The results of this study have provided a plausible rationale for the differences in the arylative cyclization reactions of the **OPiv**- and **OMe**-substituted substrates which have been discussed in detail. Our theoretical calculations revealed that the **OPiv**- and **OMe**-substituted substrates experienced the same N−H deprotonation, C−H activation (via a concerted CMD process), and 1,6-enyne insertion steps. However, starting from the seven-membered rhodacycles, the nature of the OR substituent has a significant impact on the outcome of the reaction.

For the reaction of the **OPiv**-containing substrate, a change in the coordination of the pivalate ligand to the Rh center from a bidentate to a monodentate ligand is followed by a C−N bond-forming reductive elimination step to give a Rh(I) intermediate. The subsequent migration of the **OPiv** group

DOI: 10.1021/acs.joc.5b02747
J. Org. Chem. 2016, 81, 1921−1929

from the N atom to the Rh atom would be followed by the Ⓝ-Michael addition. The final step in this process would be a protonation from pivalic acid to allow for the regeneration of the catalyst and the concomitant release of the tetracyclic isoquinolone product. The cleavage of the N−O bond from the seven-membered rhodacycles (i.e., Rh(III) → Rh(V)) is energetically unfavorable.

For the reaction of the **OMe**-substituted substrate, the seven-membered rhodacycle was determined to be unstable and therefore readily coordinated by the double bond of the cyclohexadienone. The subsequent ©-Michael addition step is followed by the protonation of the internal oxidant by pivalic acid. The dissociation of the internal oxidant from the Rh center then occurs, which is readily protonated by pivalic acid to regenerate **A** with the concomitant release of the hydrobenzofuran product.

■ ASSOCIATED CONTENT

Ⓢ Supporting Information

The Supporting Information is available free of charge on the ACS Publications website at DOI: 10.1021/acs.joc.5b02747.

Complete ref 18, calculated imaginary frequencies of all transition state species, and tables of Cartesian coordinates and electronic energies for all of the calculated structures (PDF)

■ AUTHOR INFORMATION

Corresponding Author

*E-mail: tchjli@jnu.edu.cn.

Notes

The authors declare no competing financial interest.

■ ACKNOWLEDGMENTS

This work was supported by the National Natural Science Foundation of China (Grant No. 21573095), the Fundamental Research Funds for the Central Universities (Grant No. 21615405), and the high-performance computing platform of Jinan University.

■ REFERENCES

(1) For selected reviews, see: (a) Ackermann, L. *Chem. Rev.* **2011**, *111*, 1315−1345. (b) Yeung, C. S.; Dong, V. M. *Chem. Rev.* **2011**, *111*, 1215−1292. (c) Baudoin, O. *Chem. Soc. Rev.* **2011**, *40*, 4902−4911. (d) Cho, S. H.; Kim, J. Y.; Kwak, J.; Chang, S. *Chem. Soc. Rev.* **2011**, *40*, 5068−5083. (e) Wencel-Delord, J.; Dröge, T.; Liu, F.; Glorius, F. *Chem. Soc. Rev.* **2011**, *40*, 4740−4761. (f) Li, B.-J.; Shi, Z.-J. *Chem. Soc. Rev.* **2012**, *41*, 5588−5598. (g) Engle, K. M.; Mei, T.-S.; Wasa, M.; Yu, J.-Q. *Acc. Chem. Res.* **2012**, *45*, 788−802. (h) Neufeldt, S. R.; Sanford, M. S. *Acc. Chem. Res.* **2012**, *45*, 936−946. (i) Arockiam, P. B.; Bruneau, C.; Dixneuf, P. H. *Chem. Rev.* **2012**, *112*, 5879−5918. (j) Kuhl, N.; Hopkinson, M. N.; Wencel-Delord, J.; Glorius, F. *Angew. Chem., Int. Ed.* **2012**, *51*, 10236−10254.

(2) Reviews on Rh-catalyzed C−H activation: (a) Satoh, T.; Miura, M. *Chem. - Eur. J.* **2010**, *16*, 11212−11222. (b) Kuhl, N.; Schröder, N.; Glorius, F. *Adv. Synth. Catal.* **2014**, *356*, 1443−1460. (c) Wendlandt, A. E.; Suess, A. M.; Stahl, S. S. *Angew. Chem., Int. Ed.* **2011**, *50*, 11062−11087. (d) Ye, B.; Cramer, N. *Acc. Chem. Res.* **2015**, *48*, 1308−1318. (e) Song, G.; Wang, F.; Li, X. *Chem. Soc. Rev.* **2012**, *41*, 3651−3678. (f) Colby, D. A.; Tsai, A. S.; Bergman, R. G.; Ellman, J. A. *Acc. Chem. Res.* **2012**, *45*, 814−825.

(3) (a) Chatani, N. *Topics in Organometallic Chemistry: Directed Metallation*; Springer-Verlag: Berlin, Germany, 2007; Vol. *24*. (b) Murai, S.; Kakiuchi, F.; Sekine, S.; Tanaka, Y.; Kamatani, A.; Sonoda, M.; Chatani, N. *Nature* **1993**, *366*, 529−531. (c) Ros, A.; Fernández, R.; Lassaletta, J. M. *Chem. Soc. Rev.* **2014**, *43*, 3229−3243. (d) Zhang, F.; Spring, D. R. *Chem. Soc. Rev.* **2014**, *43*, 6906−6919.

(4) (a) Mo, J.; Wang, L.; Liu, Y.; Cui, X. *Synthesis* **2015**, *47*, 439−459. (b) Huang, H.; Ji, X.; Wu, W.; Jiang, H. *Chem. Soc. Rev.* **2015**, *44*, 1155−1171. (c) Patureau, F. W.; Glorius, F. *Angew. Chem., Int. Ed.* **2011**, *50*, 1977−1979.

(5) For some recent examples, see: (a) Yu, S.; Liu, S.; Lan, Y.; Wan, B.; Li, X. *J. Am. Chem. Soc.* **2015**, *137*, 1623−1631. (b) Zhang, X.; Qi, Z.; Li, X. *Angew. Chem., Int. Ed.* **2014**, *53*, 10794−10798. (c) Hyster, T. K.; Dalton, D. M.; Rovis, T. *Chem. Sci.* **2015**, *6*, 254−258. (d) Piou, T.; Rovis, T. *J. Am. Chem. Soc.* **2014**, *136*, 11292−11295. (e) Neely, J. M.; Rovis, T. *J. Am. Chem. Soc.* **2014**, *136*, 2735−2738. (f) Fan, Z.; Song, S.; Li, W.; Geng, K.; Xu, Y.; Miao, Z.-H.; Zhang, A. *Org. Lett.* **2015**, *17*, 310−313. (g) Muralirajan, K.; Haridharan, R.; Prakash, S.; Cheng, C.-H. *Adv. Synth. Catal.* **2015**, *357*, 761−766. (h) Wu, S.; Zeng, R.; Fu, C.; Yu, Y.; Zhang, X.; Ma, S. *Chem. Sci.* **2015**, *6*, 2275−2285. (i) Zhang, H.; Wang, K.; Wang, B.; Yi, H.; Hu, F.; Li, C.; Zhang, Y.; Wang, J. *Angew. Chem., Int. Ed.* **2014**, *53*, 13234−13238.

(6) For reviews, see: (a) Patureau, F. W.; Wencel-Delord, J.; Glorius, F. *Aldrichimica Acta* **2012**, *45*, 31−41. (b) Hu, F.; Xia, Y.; Ma, C.; Zhang, Y.; Wang, J. *Chem. Commun.* **2015**, *51*, 7986−7995.

(7) For selected examples, see: (a) Huckins, J. R.; Bercot, E. A.; Thiel, O. R.; Hwang, T.-L.; Bio, M. M. *J. Am. Chem. Soc.* **2013**, *135*, 14492−14495. (b) Zhao, D.; Shi, Z.; Glorius, F. *Angew. Chem., Int. Ed.* **2013**, *52*, 12426−12429. (c) Hesp, K. D.; Bergman, R. G.; Ellman, J. A. *J. Am. Chem. Soc.* **2011**, *133*, 11430−11433. (d) Zhou, B.; Hou, W.; Yang, Y.; Li, Y. *Chem. - Eur. J.* **2013**, *19*, 4701−4706. (e) Bera, M.; Maji, A.; Sahoo, S. K.; Maiti, D. *Angew. Chem., Int. Ed.* **2015**, *54*, 8515−8519. (f) Hermann, G. N.; Becker, P.; Bolm, C. *Angew. Chem., Int. Ed.* **2015**, *54*, 7414−7417. (g) Wang, Z.; Kuninobu, Y.; Kanai, M. *J. Am. Chem. Soc.* **2015**, *137*, 6140−6143.

(8) For selected theoretical examples, see: (a) Sun, H.; Wang, C.; Yang, Y.-F.; Chen, P.; Wu, Y.-D.; Zhang, X.; Huang, Y. *J. Org. Chem.* **2014**, *79*, 11863−11872. (b) Zhang, Q.; Yu, H.-Z.; Li, Y.-T.; Liu, L.; Huang, Y.; Fu, Y. *Dalton Trans.* **2013**, *42*, 4175−4184. (c) Algarra, A. G.; Cross, W. B.; Davies, D. L.; Khamker, Q.; Macgregor, S. A.; McMullin, C. L.; Singh, K. *J. Org. Chem.* **2014**, *79*, 1954−1970. (d) Yu, H.; Lu, Q.; Dang, Z.; Fu, Y. *Chem. - Asian J.* **2013**, *8*, 2262−2273.

(9) (a) Fukui, Y.; Liu, P.; Liu, Q.; He, Z.-T.; Wu, N.-Y.; Tian, P.; Lin, G.-Q. *J. Am. Chem. Soc.* **2014**, *136*, 15607−15614. (b) Tello-Aburto, R.; Harned, A. M. *Org. Lett.* **2009**, *11*, 3998−4000. (c) Cai, S.; Liu, Z.; Zhang, W.; Zhao, X.; Wang, D. Z. *Angew. Chem., Int. Ed.* **2011**, *50*, 11133−11137. (d) Keilitz, J.; Newman, S. G.; Lautens, M. *Org. Lett.* **2013**, *15*, 1148−1151. (e) He, Z.-T.; Tian, B.; Fukui, Y.; Tong, X.; Tian, P.; Lin, G.-Q. *Angew. Chem., Int. Ed.* **2013**, *52*, 5314−5318. (f) Liu, P.; Fukui, Y.; Tian, P.; He, Z.-T.; Sun, C.-Y.; Wu, N.-Y.; Lin, G.-Q. *J. Am. Chem. Soc.* **2013**, *135*, 11700−11703. (g) Takenaka, K.; Mohanta, S. C.; Sasai, H. *Angew. Chem., Int. Ed.* **2014**, *53*, 4675−4679.

(10) (a) Xu, L.; Zhu, Q.; Huang, G.; Cheng, B.; Xia, Y. *J. Org. Chem.* **2012**, *77*, 3017−3024. (b) Guo, W.; Zhou, T.; Xia, Y. *Organometallics* **2015**, *34*, 3012−3020. (c) Zhou, T.; Guo, W.; Xia, Y. *Chem. - Eur. J.* **2015**, *21*, 9209−9218. (d) Guo, W.; Xia, Y. *J. Org. Chem.* **2015**, *80*, 8113−8121.

(11) (a) Zhao, Y.; Schultz, N. E.; Truhlar, D. G. *J. Chem. Phys.* **2005**, *123*, 161103. (b) Zhao, Y.; Truhlar, D. G. *Acc. Chem. Res.* **2008**, *41*, 157−167. (c) Zhao, Y.; Truhlar, D. G. *Theor. Chem. Acc.* **2008**, *120*, 215−241. (d) Zhao, Y.; Truhlar, D. G. *J. Chem. Theory Comput.* **2009**, *5*, 324−333.

(12) (a) Fukui, K. *J. Phys. Chem.* **1970**, *74*, 4161−4163. (b) Fukui, K. *Acc. Chem. Res.* **1981**, *14*, 363−368.

(13) (a) Hay, P. J.; Wadt, W. R. *J. Chem. Phys.* **1985**, *82*, 299−310. (b) Wadt, W. R.; Hay, P. P. J. *J. Chem. Phys.* **1985**, *82*, 284−298.

(14) Ehlers, A. W.; Böhme, M.; Dapprich, S.; Gobbi, A.; Höllwarth, A.; Jonas, V.; Köhler, K. F.; Stegmann, R.; Veldkamp, A.; Frenking, G. *Chem. Phys. Lett.* **1993**, *208*, 111−114.

(15) Hariharan, P. C.; Pople, J. A. *Theor. Chim. Acta.* **1973**, *28*, 213−222.

(16) Marenich, A. V.; Cramer, C. J.; Truhlar, D. G. *J. Phys. Chem. B* **2009**, *113*, 6378−6396.

DOI: 10.1021/acs.joc.5b02747
J. Org. Chem. 2016, 81, 1921−1929

(17) (a) Fuentealba, P.; Preuss, H.; Stoll, H.; Vonszentpaly, L. *Chem. Phys. Lett.* **1982**, *89*, 418. (b) von Szentpaly, L.; Fuentealba, P.; Preuss, H.; Stoll, H. *Chem. Phys. Lett.* **1982**, *93*, 555. (c) Fuentealba, P.; Stoll, H.; Szentpaly, L. V.; Schwerdtfeger, P.; Preuss, H. *J. Phys. B: At. Mol. Phys.* **1983**, *16*, L323.
(18) Frisch, M. J. *Gaussian 09*, revision C.01; Gaussian, Inc.: Wallingford, CT, 2010. Full reference given in Supporting Information.
(19) A Rh(III)/Rh(I) catalytic cycle is demonstrated for Rh(III)-catalyzed C−H activation of 2-acetyl-1-arylhydrazines with the alkynes as the coupling partner: Chen, W.-J.; Lin, Z. *Organometallics* **2015**, *34*, 309−318.
(20) See the Supporting Information for more computational details (Figure S2).
(21) The reaction selectivity for **OPiv** and **OMe** systems according to the gas-phase energies were consistent with that according to the solvent-corrected energies.

DOI: 10.1021/acs.joc.5b02747
J. Org. Chem. 2016, 81, 1921−1929